

Effect of excess selenium in the formation of $\text{Cu}_2\text{Zn}_{1.5}\text{Sn}_{1.2}(\text{S}_{0.9}+\text{Se}_{0.1})_4$ alloys for solar cell applications

Chinnaiyah Sripan¹, Annamraju Kasi Viswanath¹, Ganesan R.²

¹Centre for Nanoscience and Technology, Pondicherry University, Pondicherry, India

²Department of Physics, Indian Institute of Science, Bangalore, Karnataka, India

Srimannano2007@gmail.com, v_kasi@hotmail.com, rajamanickam.ganesan@gmail.com

PACS 81.05.Bx, 88.05.Ec, 81.05.Hd

DOI 10.17586/2220-8054-2016-7-3-509-512

Copper zinc tin sulfide/selenide $\text{Cu}_2\text{ZnSn}(\text{S}, \text{Se})_4$ (CZTSSe) is an alternative promising material for solar cell applications. It exhibits a high optical absorbance and tunable band gap. We have investigated the effect of excess selenium on the formation of CZTSSe phase which was prepared by the thermal melt method. The CZTSSe alloys were characterized by X-ray diffraction (XRD), Raman spectroscopy and UV-VIS spectroscopy. The crystallographic structure and phase were confirmed by X-ray diffraction and Raman spectroscopic techniques. In Raman spectroscopy, we found that the phase shifts from 327 cm^{-1} to 338 cm^{-1} when the selenium content excess is 5 %. In optical studies, a band gap for the CZTSSe alloys of about 1.43 eV to 1.44 eV was observed.

Keywords: $\text{Cu}_2\text{ZnSn}(\text{S}, \text{Se})_4$, raman spectroscopy, solar cell.

Received: 2 February 2016

Revised: 18 April 2016

1. Introduction

The development of clean energy resources as an alternative to fossil fuels has become one of the most important tasks assigned to current researchers. Recently, photovoltaic devices based on several semiconductor nanocrystal (NCs), including CdTe, Cu(In,Ga)Se₂ and Cu(In,Ga)S₂ have been realized. Through this research, technologies have reached commercial module production with power conversion efficiencies of up to 9 %, however, their potential is restricted by the limited supply of In and Ga as well as by restrictions on the safe usage of Cd. $\text{Cu}_2\text{ZnSnS}_4$ (CZTS) and $\text{Cu}_2\text{ZnSnSe}_4$ (CZTSe) are two promising materials for Photovoltaic applications. Copper-Indium-Gallium-Selenide/Sulfide (CIGS) solar cells have achieved about 20 % conversion efficiency at the laboratory scale, which is one of the highest efficiency among various thin film solar cells. However, CIGS solar cells adopt rare earth elements. In this point of view $\text{Cu}_2\text{ZnSn}(\text{S},\text{Se})_4$ (CZTSSe) is a very promising absorber material [1–4]. It includes earth abundant elements Sn, Zn, moreover less toxic S and Se. In addition, the CZTSSe exhibits excellent optical properties such as a direct band gap of 1.1 to 1.5 eV and a large absorption coefficient of 10^4 cm^{-1} in visible spectrum range. CZTS thin film has been prepared by various methods such as vacuum based synthesis and solution based synthesis. Band gap of CZTSSe thin film can be tuned by controlling the stoichiometry of the reactants. In this material, the theoretically predicted power conversion is 32.2 %, but in experiments they have achieved 6.77 % efficiency by vacuum-based process [5] and 12.6 % by another solution process. However the device performance was greatly improved, basic research on CZTSSe material itself are insufficient, for example fabrication of compositionally-uniform CZTSSe film is still hard task due to the loss of Sn during the annealing process [7]. Considering that high efficiency solar cell can be realized just with Cu poor and Zn rich CZTS [8], careful and precise adjustment of chemical compositions of CZTS is prerequisite. Based on this research, we adjusted the stoichiometry of $\text{Cu}/(\text{Zn}+\text{Sn})=0.77$ and $\text{Zn}/\text{Sn}=1.25$ for much-improved grain size. Hence, the systematic sulfurization and experiments under controlled temperature and surrounding atmosphere came to be significant.

2. Experimental methods

Polycrystalline alloys $\text{Cu}_2\text{Zn}_{1.5}\text{Sn}_{1.2}(\text{S}_{0.9}+\text{Se}_{0.1})_4$, (without excess selenium) $\text{Cu}_2\text{Zn}_{1.5}\text{Sn}_{1.2}(\text{S}_{0.9}+\text{Se}_{0.105})_4$ – 5 % of excess Se, $\text{Cu}_2\text{Zn}_{1.5}\text{Sn}_{1.2}(\text{S}_{0.9}+\text{Se}_{0.110})_4$ – 10 % of excess Se and $\text{Cu}_2\text{Zn}_{1.5}\text{Sn}_{1.2}(\text{S}_{0.9}+\text{Se}_{0.115})_4$ – 15 % of excess Se were prepared by a thermal melt technique using separate single source materials. The single source materials were prepared by taking elements in stoichiometry ratio of 2.0:1.5:1.2:4. Pure elements of Cu, Zn, Sn, S and Se (99.999 % Alfa Aesar) were weighed in atomic stoichiometry ratio and transferred to meticulously-cleaned quartz ampoule. The ampoules were sealed at 1×10^{-5} mbar vacuum and this ampoule was placed in electric furnace and slowly heated at 500 °C (5 °C/min) and kept at that temperature for one hour. The temperature was

then increased to 950 °C. To ensure the homogeneity of the molten materials, the ampoules were rotated for 24 hrs at this temperature and gradually cooled to room temperature.

2.1. Material characterizations

The structural analysis of the base material powder was done by XRD using Cu-K α source (wavelength=1.5405 Å) with a diffraction angle from 10 ° to 80 ° degree (BRUKER D8-ADVANCE). The investigation of the phase formation of CZTSe bulk materials were characterized by Raman spectroscopy using the excitation wavelength of 532 nm (HORIBA Jobin YVON Lab RAM HR800 spectrometer). The UV-Visible spectra of CZTSe alloy materials were recorded by Perkin Elmer UV/Visible spectrometer Lambda 35 from 400 – 1100 nm.

3. Results and discussion

The structures of the as-synthesized alloys were characterized by XRD, as show in Fig. 1a and 1b. The diffraction peaks of as-prepared CZTSSe alloys can be indexed to pure phase of kesterite structure (CZTSSe) (ICSD No-184475). The major diffraction peak appeared at 2θ 28.23 °, 32.3 °, 47.27 ° and 55.8 ° attributed to (112), (200), (220) and (312) hkl planes, can be seen clearly. The lattice parameters $a = b = 5.62$ Å, $c = 11.22$ Å of the typical sample were similar to that described in the literature [8,9]. Also, the secondary peaks SnSe and ZnS presented all excess selenium presented alloys. But in excess selenium content 5 % the intensity of SnSe and ZnS was much less compared to the 0 % and 10 % excess selenium.

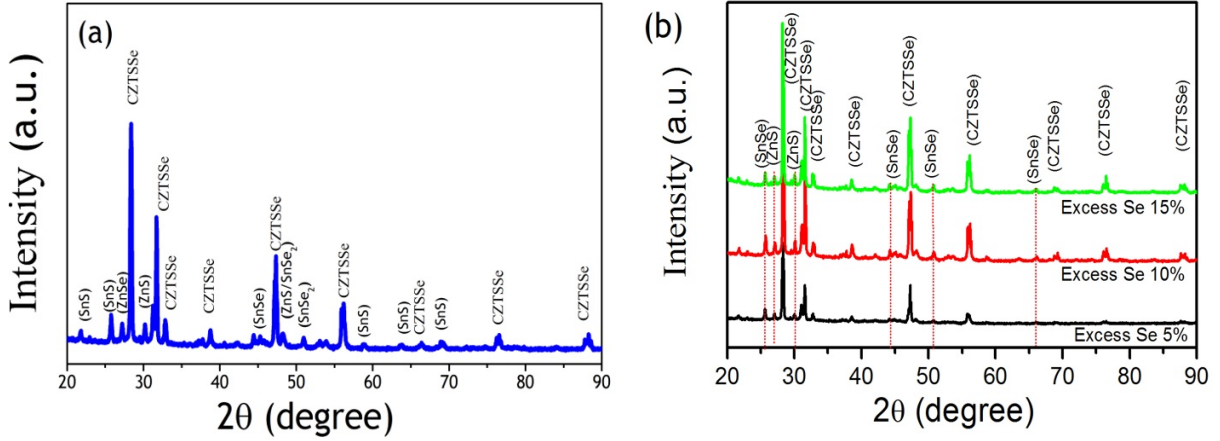


FIG. 1. X-ray diffraction (XRD) pattern of synthesized CZTSSe alloys. (a) $\text{Cu}_2\text{Zn}_{1.5}\text{Sn}_{1.2}(\text{S}_{0.9}+\text{Se}_{0.1})_4$ alloy, (b) 5, 10 and 15 % of excess selenium alloys

Also, we have noted the differentiation of (112) diffraction peaks shift for alloys of no excess selenium alloy and 5 % excess selenium. Fig. 2 shows that the diffraction peak shifted from smaller 2θ values to higher 2θ values as the selenium content increases, indicating the replacement of sulfur with selenium [10]. The Raman spectra of $\text{Cu}_2\text{Zn}_{1.5}\text{Sn}_{1.2}(\text{S}_{0.9}+\text{Se}_{0.1})_4$ and $\text{Cu}_2\text{Zn}_{1.5}\text{Sn}_{1.2}(\text{S}_{0.9}+\text{Se}_{0.105})_4$ (5 % excess selenium) bulk materials are shown in Fig. 3. In bulk materials, the primary vibration of $\text{Cu}_2\text{Zn}_{1.5}\text{Sn}_{1.2}(\text{S}_{0.9}+\text{Se}_{0.1})_4$ was detected at 327 cm^{-1} and 197 cm^{-1} due to selenium-selenium vibration, but could not detected secondary phases, which might be due to the difference in sensitivity or the minute presence of CZTSSe alloys. In $\text{Cu}_2\text{Zn}_{1.5}\text{Sn}_{1.2}(\text{S}_{0.9}+\text{Se}_{0.105})_4$ (5 % excess selenium) alloy the primary peaks were detected at 337 cm^{-1} , 287 cm^{-1} and 367 cm^{-1} for CZTS and 197 cm^{-1} and 239 cm^{-1} for CZTSe. The peak shifted from lower wave number to higher wave numbers [10].

The optical band gap (E_g) for $\text{Cu}_2\text{Zn}_{1.5}\text{Sn}_{1.2}(\text{S}_{0.9}+\text{Se}_{0.1})_4$ and $\text{Cu}_2\text{Zn}_{1.5}\text{Sn}_{1.2}(\text{S}_{0.9}+\text{Se}_{0.105})_4$ (5 % excess selenium) alloys were calculated where the absorbance co-efficient value was $> 10^4\text{ cm}^{-1}$. The optical band gap of material was determined by the Tauc and the Davis and Mott models [11]. This is shown in Fig. 4:

$$(\alpha h\nu) = B(h\nu - E_g)^n,$$

where B is constant (Tauc parameter), h is Planck's constant, ν is frequency, E_g is optical band gap and n is a number which related mechanism of transition process, the value of n is taken to be $1/2$ for direct transition. In an alloy without excess selenium, a band gap of 1.44 eV was obtained experimentally. For $\text{Cu}_2\text{Zn}_{1.5}\text{Sn}_{1.2}(\text{S}_{0.9}+\text{Se}_{0.105})_4$ (5 % excess selenium) alloy, the band gap decreased to 1.43 eV. The reduction in the number of unsaturated defects, which decreases the density of localized states in the band structure and consequently decreases the optical band gap, may be attributable to an excess of selenium present.

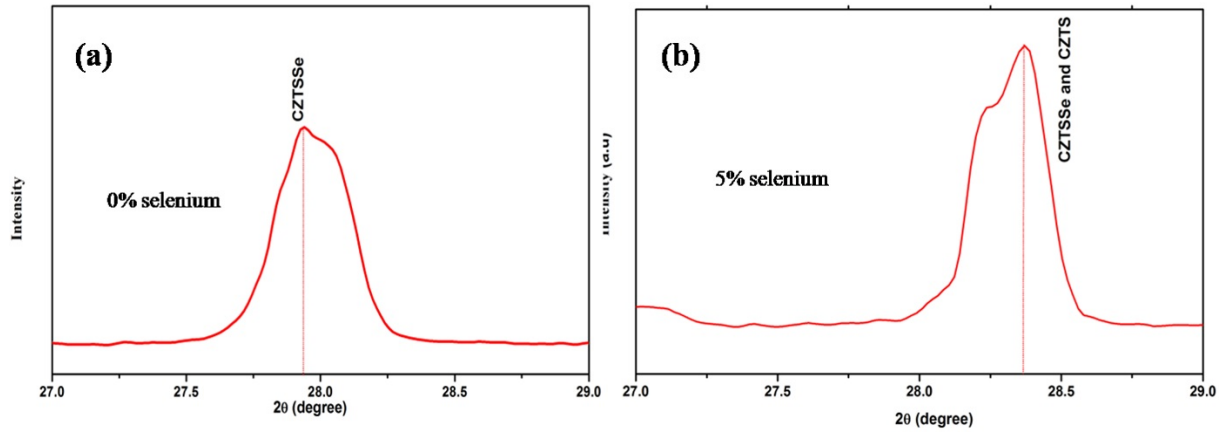


FIG. 2. X-ray diffraction (XRD) pattern- differentiates the peak shift of $\text{Cu}_2\text{Zn}_{1.5}\text{Sn}_{1.2}(\text{S}_{0.9}+\text{Se}_{0.1})_4$ and $\text{Cu}_2\text{Zn}_{1.5}\text{Sn}_{1.2}(\text{S}_{0.9}+\text{Se}_{0.105})_4$ alloys

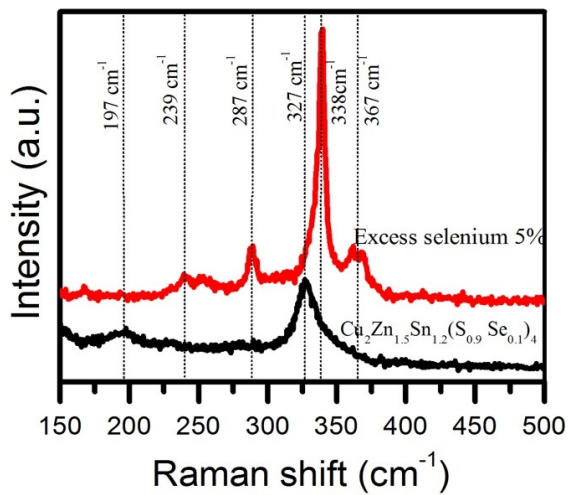


FIG. 3. Raman spectroscopy of CZTSSe alloys in different excess selenium

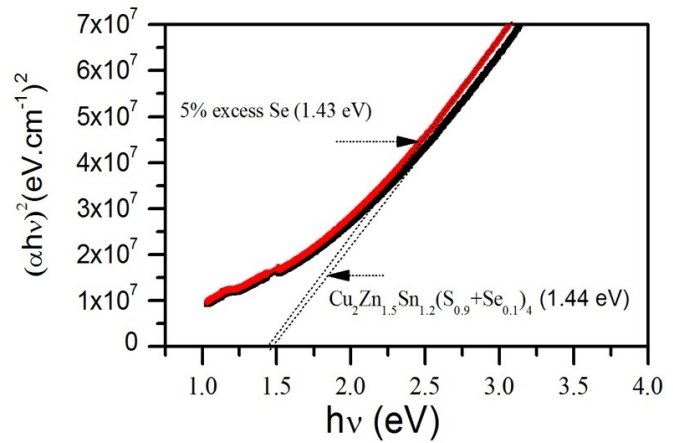


FIG. 4. Optical band gap of CZTSSe alloys in different excess selenium

4. Conclusion

We have investigated the effect of excess selenium on the formation of CZTSSe phase prepared via the thermal melt method. The crystallographic structures of CZTSSe alloys phase were confirmed by X-ray diffraction and Raman spectroscopic techniques. In Raman spectroscopic analyses, we found that the phase shifts from 327 cm^{-1} to 338 cm^{-1} when the selenium content is 5 % in excess. In optical studies, we have found the band gap for CZTSSe alloys to be about 1.43 – 1.44 eV.

Acknowledgement

The authors thank Inorganic and Physical Chemistry (IPC-IISc, Bangalore) and Department of Physics (IISc, Bangalore) for XRD and UV-Visible characterizations.

References

- [1] Ito K., Nakazawa T. Direct Liquid Coating of Chalcopyrite Light-Absorbing Layers for Photovoltaic Devices. *Jpn. J. Appl. Phys.*, 1988, **27**(1), P. 2094–2097.
- [2] Katagiri H., Saitoh K., et al. Miyajima Development of thin film solar cell based on $\text{Cu}_2\text{ZnSnS}_4$ thin films. *Sol. Energy Mater. Sol. Cells*, 2001, **65**(1), P. 141–148.
- [3] Seol J.S., Lee S.Y., et al. Electrical and optical properties of $\text{Cu}_2\text{ZnSnS}_4$ thin films prepared by rf magnetron sputtering process. *Sol. Energy Mater. Sol. Cells*, 2003, **75**(1), P. 155–162.

- [4] Katagiri H., Jimbo K., et al. Development of CZTS-based thin film solar cells. *Thin Solid Films*, 2009, **517**(7), P. 2455–2460.
- [5] Katagiri H., Jimbo K., et al. Enhanced Conversion Efficiencies of $\text{Cu}_2\text{ZnSnS}_4$ -Based Thin Film Solar Cells by Using Preferential Etching Technique. *Appl. Phys. Express*, 2008, **1**(4), P. 041201.
- [6] Todorov T.K., Reuter K.B., Mitzi D.B. Photovoltaic Devices: High-Efficiency Solar Cell with Earth-Abundant Liquid-Processed Absorber. *Adv. Mater* 2010, **22**(20), P. E156-9.
- [7] Weber A., Mainz R., Schock H.W. On the Sn loss from thin films of the material system Cu–Zn–Sn–S in high vacuum. *J. Appl. Phys*, 2010, **107**(1), P. 013516.
- [8] Mitzi D.B., Gunawan O.i., et al. The path towards a high-performance solution-processed kesterite solar cell. *Sol. Energy Mater. Sol. Cells*, 2011, **95**(6), P. 1421–1436.
- [9] Jiang C., Lee J.-S., Talapin D.V. Soluble Precursors for CuInSe_2 , $\text{CuIn}_{1-x}\text{Ga}_x\text{Se}_2$, and $\text{Cu}_2\text{ZnSn}(\text{S},\text{Se})_4$ Based on Colloidal Nanocrystals and Molecular Metal Chalcogenide Surface Ligands. *J. Am. Chem. Soc.*, 2012, **134**(11), P. 5010–5013.
- [10] Yang W., Duan H.-S., et al. Novel Solution Processing of High-Efficiency Earth-Abundant $\text{Cu}_2\text{ZnSn}(\text{S},\text{Se})_4$ Solar Cells. *Adv. Mater* 2012, **24**(47), P. 6323–6329.
- [11] Fischereder A., Rath T., et al. Investigation of $\text{Cu}_2\text{ZnSnS}_4$ Formation from Metal Salts and Thioacetamide. *Chem. Mater*, 2010, **22**(11), P. 3399–3406.